

Accepted Manuscript

Seven coordinated cobalt(II) complexes with 2,6-diacetylpyridine bis(4-acylhydrazone) ligands: Synthesis, characterization, DNA-binding and nuclease activity

Cansu Gökçe, Nefise Dilek, Ramazan Gup

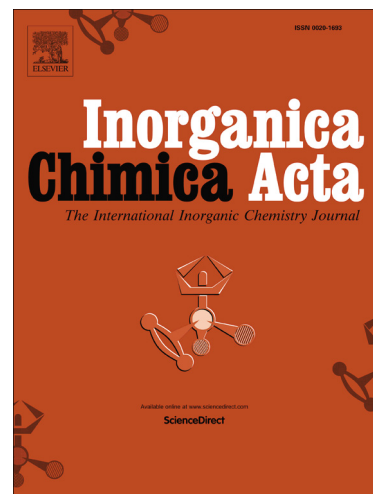
PII: S0020-1693(15)00189-9
DOI: <http://dx.doi.org/10.1016/j.ica.2015.03.040>
Reference: ICA 16494

To appear in: *Inorganica Chimica Acta*

Received Date: 5 December 2014
Revised Date: 24 March 2015
Accepted Date: 28 March 2015

Please cite this article as: C. Gökçe, N. Dilek, R. Gup, Seven coordinated cobalt(II) complexes with 2,6-diacetylpyridine bis(4-acylhydrazone) ligands: Synthesis, characterization, DNA-binding and nuclease activity, *Inorganica Chimica Acta* (2015), doi: <http://dx.doi.org/10.1016/j.ica.2015.03.040>

This is a PDF file of an unedited manuscript that has been accepted for publication. As a service to our customers we are providing this early version of the manuscript. The manuscript will undergo copyediting, typesetting, and review of the resulting proof before it is published in its final form. Please note that during the production process errors may be discovered which could affect the content, and all legal disclaimers that apply to the journal pertain.



Seven coordinated cobalt(II) complexes with 2,6-diacetylpyridine bis(4-acylhydrazone) ligands: Synthesis, characterization, DNA-binding and nuclease activity

Cansu Gökçe^a, Nefise Dilek^b and Ramazan Gup^{a*}

^a*Department of Chemistry, Science Faculty, Mugla Sıtkı Koçman University, 48100, Mugla, Turkey*

^b*Department of Physics, Arts and Sciences Faculty, Aksaray University, 68100, Aksaray, Turkey*

ABSTRACT

A new series of pentadentate 2,6-diacetylpyridine bis(4-acylhydrazone)s (H_2L^1 and H_2L^2) based seven-coordinated cobalt(II) complexes, $[Co(L^n)X_2]$ ($n= 1$ and $X= DMF$ for **(1)**; $n= 2$ and $X= H_2O$ for **(2)**); $[Co(H_2L^n)Y_2]$ ($n= 1$ or 2 ; $Y= N_3^-$ or NCS^-), has been synthesized and characterized by using spectroscopic techniques. Single crystal X-ray study of $[Co(L^1)(DMF)_2]$ (**(1)**) complex exhibits pentagonal-bipyramidal coordination geometry where the pentadentate N_3O_2 ligand in the equatorial plane of the bipyramid and two dimethylformamide molecules in the axial area. Interaction of the cobalt(II) complexes with CT DNA has been investigated by absorption titration method and viscosity measurements which reveal that the cobalt(II) complexes could bind with CT DNA through intercalation. Cleavage activity of the complexes **(1)** and **(2)** with pBR 322 plasmid DNA was evaluated by agarose gel electrophoresis demonstrating that the ability of the complexes to cleave the pBR 322 plasmid DNA *via* oxidative pathway, possibly due to the involvement of a diffusible hydroxyl radical mechanism in presence and absence of an oxidative agent. The nuclease activity of the Co(II) complexes has strong dependence on the concentration of complex and reaction time, both in presence and absence of hydrogen peroxide.

Keywords: 2,6-Diacetylpyridine; acylhydrazone; cobalt(II) complex; DNA binding; nuclease activity

1. Introduction

Transition metal complexes have a huge impact on biological applications in bioinorganic chemistry due to their coordination behavior and importance in catalysis [1-6]. The interaction of transition metal complexes with DNA has been intensively studied to develop newer materials for application in biotechnology and medicine in recent years. Generally, DNA is the essential target molecule for most disease therapies such as anticancer and antiviral. Any disorder in gene expression may cause diseases and plays a secondary role in the outcome and severity of human diseases. Transition metal complexes can interact with DNA through the covalent or non-covalent modes such as groove binding, intercalation and external static electronic effects among them the most important is intercalation [7,8]. Investigations have resulted in the synthesis of many new transition metal based complexes, which bind to DNA through non-covalent interactions [8-12]. Cleavage of DNA may be considered as an enzymatic reaction which comprises various biological processes as well as biotechnical manipulation of genetic material. Thus, there is an increasing focus on the interaction study of small molecules with DNA during the last decades. A more complete understanding of DNA binding is necessary to design a new drug.

Geometry of the coordination compounds depending on the metal ion type and different functional groups in the ligands is primarily responsible for the affinity of the metal complexes to DNA. Transition metal complexes with tunable coordination environments offer a great scope for the design of species that are suitable for DNA binding and cleavage activities. Although many cobalt complexes with different geometries have been synthesized, characterized and their interactions with DNA have been studied extensively [8,9,12-18], there is no report related to DNA binding and DNA cleavage studies of seven coordinated cobalt complexes in literature, to the best of our knowledge. A few heptacoordinate Co(II) complexes based on bis(acylhydrazone) ligands have been synthesized and characterized. Giordano et al., design and synthesized a seven-coordinated Co(II) complex $[\text{Co}(\text{H}_2\text{DAPBH})(\text{H}_2\text{O})(\text{NO}_3)](\text{NO}_3)$ [H_2DAPBH = 2,6-diacetylpyridine bis-(benzoylhydrazone)] [19] and Ruamps and co-workers [20] investigated the nature and magnitude of the magnetic anisotropy of this complex by a combination of experiment and ab initio calculations. On the other hand, many seven coordinated metal complexes based on 2,6-diacetylpyridine bis(hydrazone) ligands have been synthesized and characterized [21-27], yet only a few of them have

reported on their pharmacological properties and RNA interactions. So here in, we report the synthesis and characterization and DNA interaction of the new seven coordinated Co(II) complexes of two 2,6-diacetylpyridine pentadentate bis(acylhydrazone) ligands bearing carboxylic acid ester groups.

2. Results and discussion

The new pentadentate hydrazone Schiff base ligands containing carboxylic ester groups, 2,6-diacetylpyridine bis(4-ethoxyacetatebenzoylhydrazone) (H_2L^1) and 2,6-diacetylpyridine bis(4-ethoxybutyratebenzoylhydrazone) (H_2L^2), were easily prepared by the reaction of 2,6-diacetylpyridine bis(4-hydroxybenzoylhydrazone) with ethyl bromoacetate and ethyl 4-bromobutyrate in the presence of dry K_2CO_3 and catalytic amount of KI. The cobalt(II) complexes were synthesized by the reaction of the synthesized Schiff base hydrazone ligands with cobalt(II) acetate and unidentate ion in the ratio of 1:1:2. The nature of bonding and geometry of the Co(II) complexes as well as Schiff base hydrazones were deduced from elemental analysis, magnetic susceptibility measurements, various spectroscopies (IR, UV-Vis, 1H NMR, ^{13}C NMR) and single crystal X ray diffraction techniques.

2.1. NMR spectra

The main 1H NMR signals for each of the H_2L^1 and H_2L^2 ligands in DMSO- d_6 are given in the experimental section. Formations of the H_2L^1 and H_2L^2 are confirmed by the absence of the OH proton signal at 10.16 ppm assigned to the starting material 2,6-diacetylpyridine bis(4-hydroxybenzoylhydrazone). In the ^{13}C NMR spectra of ligands, the signals for the carbonyl carbons of carboxylic ester and amide groups are observed at 170.4 and 161.7 for H_2L^2 and 168.4 and 154.2 ppm for H_2L^1 . The characteristic chemical shifts of azomethine groups appear at 142.5 and 142.1 ppm. These assignments are in good agreement with those previously reported for similar compounds [27-30].

2.2. IR spectroscopy

The broad vibration band of $\nu(O-H)$, in the IR spectra of the starting material, disappears and a new strong band is observed at 1758 and 1731 cm^{-1} for H_2L^1 and H_2L^2 ,

respectively, in the IR spectrum of the hydrazone ligands due to the stretching vibration of the ester carbonyl, which is also characteristic for carboxylic esters, indicating that condensation takes place [11,28-31]. In the IR spectra of the Co(II) complexes **1** and **2**, the amide I band disappears and a new band is observed at 1603 cm^{-1} probably due to $>\text{C}=\text{N}-\text{N}=\text{C}<$ stretching vibration indicating transformation of the carbonyl group to its enolic form through keto-enol tautomerism and subsequent coordination of the enolic oxygen to cobalt(II) ion after deprotonation. The IR spectra of the other cobalt(II) complexes show sharp stretching vibrations peaks between $3383-3421\text{ cm}^{-1}$, $1627-1645\text{ cm}^{-1}$, $1601-1604\text{ cm}^{-1}$ due to $\nu(\text{N}-\text{H})$, amide I and imine groups, respectively, indicating the coordination in the keto form. In addition, the bands due to the carbonyl of the carboxylic ester vibrations remain unaltered, suggesting non-involvement of these groups in the complex formation [28-31].

On the basis of IR spectral data we can conclude that in the case of the complexes **1** and **2** the bis(arylhyazone) ligands act as di anionic O,N,N',N,O-pentadentate ligands and the sixth and seventh positions are occupied by two dimethylformamide and water molecules, respectively. On the other hand, they act as neutral O,N,N',N,O-pentadentate ligands and the axial positions are occupied by SCN^- or N_3^- anions with pentagonal-bipyramidal geometry in the other cobalt(II) complexes.

2.3. Electronic absorption spectra

In the UV-vis spectra of the bis(hydrazone) ligands two bands are observed at $\sim 214\text{ nm}$ and $\sim 312\text{ nm}$. The latter is assignable to the $n \rightarrow \pi^*$ transition. The cobalt(II) complexes in DMF exhibit two bands around 270 nm and 350 nm , and a shoulder around at 416 nm . By comparing the electronic absorption spectra of the free hydrazone ligands and their Co(II) complexes, it is observed that the maxima bands of the free ligands exhibit bathochromic shifts. The first band observed in UV-vis spectra of the cobalt(II) complexes is assignable to the aromatic ring transition $\pi \rightarrow \pi^*$. The other bands can be assigned the $n \rightarrow \pi^*$ type electronic transitions.

The observed magnetic moments values of the cobalt(II) complexes range from 4.21 to 4.31 BM. These μ_{eff} values lie in the range corresponding to three unpaired electrons for pentagonal bipyramidal geometry ($S = 3/2$) around cobalt(II), d^7 complexes.

2.4. Description of Crystal structure of $[\text{Co}(\text{L}^1)(\text{DMF})_2]$ (**1**)

The crystal structure is shown in Fig. 1 with atom-numbering scheme. Basic crystal data, description of the diffraction experiment and details of the structure refinement are given in Table 1. Selected bond distances and angles are presented in Table 2. The cobalt(II) complex **1** crystallizes in the Triclinic *P-1* space group and has a crystallographic symmetry of two-fold axis. In the asymmetric unit, there are two DMF (dimethylformamide) molecules. The central Co(II) atom is seven-coordinated with N₅O₂ coordination environment and has a pentagonal bipyramid coordination geometry. The H₂L¹ acts as a pentadentate dianionic ligand which is bound to the Co(II) ion through three nitrogen atoms [N(2), N(3) and N(4)] and two oxygen atoms [O(4) and O(5)] defining the equatorial coordination plane. The pentagonal-bipyramidal coordination geometry around cobalt atom is completed by the oxygen atoms [O(9) and O(10)] of two dimethylformamide molecules which are bound to Co(II) in axial positions. The average Co-O bond length 2.191 (2) Å. The Co-N bond lengths range from 2.157 (2) to 2.230 (2) Å. The Co-N(2) bond length is slightly smaller than those of the other two Co-N bonds.

The central angle of a regular pentagon is 72°, whereas the N4-Co-N2, N2-Co-N3, O5-Co-N4 and N3-Co-N4 angles in the titled Co(II) complex are 71.98(6)°, 70.99(7)°, 69.99(6)° and 69.59(6)°, respectively. On the other hand, the regular angle between axial and equatorial positions is 90° while the observed angles of the titled Co(II) complexes are between 85.27(6)° and 93.19(6)°. The bond angle of the O9-Co-O10 in the axial position is 177.04(6)°. These observations indicate that the complex has a slightly distorted pentagonal bipyramid geometry around cobalt(II). The all chelate rings of molecule are essentially planar. The other bond lengths and angles in the molecule are within expected ranges, and similar to the other studies [19,20].

Insert Table 1

The H atoms were positioned geometrically, with C-H = 0.93 Å (aromatic) and constrained to ride on their parent atoms, with $U_{\text{iso}}(\text{H}) = 1.2U_{\text{eq}}(\text{C})$. Also, the C-bound H-atoms were positioned geometrically with C-H = 0.97 Å and 0.96 Å for methylene and methyl H-atoms, and constrained to ride on their parent atoms, with $U_{\text{iso}}(\text{H}) = 1.2U_{\text{eq}}(\text{C}_{\text{methylene}})$ and $U_{\text{iso}}(\text{H}) = 1.5U_{\text{eq}}(\text{C}_{\text{methyl}})$.

Insert Table 2

As can be seen from the packing diagram (Fig. S1), inter-molecular and intra-molecular C—H...O and C—H...N hydrogen bonds (Table S2) link the molecules and these hydrogen bonds may be effective in the stabilization of the crystal structure. In these interactions, the C32, C33, C34 and C35 atoms act as donor. Both of the DMF molecules form hydrogen bonds with the basic molecule.

2.5. Binding studies

2.5.1. Electronic absorption titrations

Fig. 2.

The interactions of cobalt(II) complexes with CT DNA were investigated by UV-Vis absorption titrations [32-34]. The electronic absorption spectra of the cobalt(II) complexes in the absence and in the increasing concentrations of CT-DNA are given in the Fig. 2 and Figs. S2-S6. The binding of the Co(II) complexes to DNA helices was characterized by following the changes in the absorbance and shift in wavelength on each addition of the increasing concentration of DNA solution to the Co(II) complex solution. Upon incremental addition of CT DNA from 0 to 80 μM , the maximum absorbance band of the cobalt(II) complexes at ~ 350 nm exhibits a significant hypochromism with a moderate blue shift of ~ 2 nm which indicates the interactions between DNA and the Co(II) complexes. The complex **1** shows the biggest hypochromism (26.29%) and hypsochromic shift (4 nm) among the all titled cobalt(II) complexes. With increasing concentration of DNA, the absorption of the complex **1** at 348 nm is almost disappeared a new shoulder appears at ~ 323 nm which affords an isobestic point at 331 nm. These spectral changes reveal that all titled Co(II) complexes interact with CT DNA most likely through an interaction mode that involves π - π stacking interaction between the aromatic chromophore and base pairs of DNA.

In order to compare the DNA binding affinity of these complexes quantitatively, their binding constants, K_b , were determined from the plot of $[\text{DNA}] / (\epsilon_a - \epsilon_f)$ versus $[\text{DNA}]$ (Table 3). The binding constant values for the cobalt(II) complexes **1**, **2**, **3**, **4**, **5** and **6** were found to be $3.33 \times 10^5 \text{ M}^{-1}$, $2.33 \times 10^5 \text{ M}^{-1}$, $2.50 \times 10^5 \text{ M}^{-1}$, $1.67 \times 10^5 \text{ M}^{-1}$, $1.00 \times 10^5 \text{ M}^{-1}$ and $2.00 \times 10^5 \text{ M}^{-1}$, respectively. The observed values of K_b reveals that the complex **1** binds more strongly to CT DNA than the other cobalt complexes via an

intercalative mode. These observations are quite similar to the K_b values of previously reported cobalt(II) complexes [12,35,36].

Insert Table 3

2.5.2. Viscosity measurements.

The binding modes of the cobalt(II) complexes to DNA were further confirmed *via* viscosity measurement carrying out by keeping $[DNA]=0.5$ mM and varying the concentrations of Co(II) complexes, DAPI or EB [28,37,38]. The results are shown in Fig. 3 and S7 – S11 for the complexes **1**, **2**, **3**, **4**, **5** and **6**, respectively. In this study, we have used the EB and DAPI as references. As can be seen from the Fig. 3, ethidium bromide (EB), being a well-known DNA intercalator between DNA base pairs and thus lengthening the DNA double helix, increases the relative viscosity of DNA sharply whereas the viscosity of double strand DNA remains almost unchanged in the case of DAPI, minor groove binding agent. An increase in the relative viscosity of CT DNA upon adding increasing amounts of cobalt(II) complexes also suggests the intercalative mode of binding.

Fig. 3.

2.6. Nuclease activity of the cobalt(II) complexes

In order to assess the nuclease activity of DNA as results of strong binding of complexes **1** and **2**, agarose gel electrophoresis was performed using supercoiled pBR322 plasmid DNA as a substrate in a medium of 5 mM Tris-HCl/50 mM NaCl buffer at pH 7.2 [38-43]. The cleavage experiments were carried out in the presence and absence of activating agent, H_2O_2 , under different concentration of complex (25-200 μ M) and incubation time (1 h to 6 h) at 37 °C, and the results are shown in Figs. 4 and 5 for **1** and Figs. S12 and S13 for **2**.

Fig. 4.

It is observed that both complexes **1** and **2** exhibit considerable nuclease activity and their DNA cleavage abilities are almost similar under both conditions. Both complexes convert the supercoiled DNA to nicked and linear forms suggesting double strand DNA cleavage. The amount of form II and III increases gradually whereas the intensity of

form I DNA diminishes with increasing concentration of the complexes. The results illustrate that the Co(II) complexes can effectively cleavage DNA both in the presence and absence an oxidative agent, and the cleavage efficiency of the complexes gradually increases with the increase in concentration of the complexes (Figs. 4a and 5a for **1**; Figs. S12a and S13a for **2**). The time course of pBR 322 DNA cleavage mediated by the cobalt(II) complexes (100 μM) was also carried out with agarose gel electrophoresis in the buffer at 37 C in presence and absence of oxidative agent. As shown in Figs. 4b, 5b, S12b and S13b, when the incubation time increases, the intensity of circular supercoiled form decreases while those of forms II and III increases gradually. In the case of the oxidative cleavage, form I is almost disappeared after 6 h incubation (lanes 6). The results illustrate that the Co(II) complexes cleavage DNA both in the presence and absence of an oxidative agent, and the cleavage of DNA by the cobalt(II) complexes is dependent on the reaction time. The results also indicate that the chemical nuclease activity of the complex **1** is slightly higher than that of the complex **2** probably due to the higher DNA binding affinity of **1**.

Fig. 5.

To elucidate the mechanism involved in the DNA cleavage by complexes **1** and **2**, the reactions were carried out in the presence of superoxide dismutase as superoxide anion radicals (O_2^-) scavenger, NaN_3 as singlet oxygen ($^1\text{O}_2$) quencher and DMSO as hydroxyl radical (OH^\bullet) scavenger in the presence and absence of hydrogen peroxide. As shown in Figs. 4c, 5c, S12c, and 13c, lanes 2, the addition of DMSO significantly inhibits the cleavage activity of the cobalt(II) complexes both in the presence and absence of H_2O_2 suggesting that the freely diffusible hydroxyl radical is involved in the DNA cleavage reaction of the Co(II) complexes **1** and **2**. It may be concluded from these results that the cobalt(II) complexes **1** and **2** may cleavage the DNA probably through oxidative mechanism.

In order to probe the potential interacting site of the cobalt(II) complexes with plasmid pBR322 DNA, the effects of groove binding drugs on the strand scission were also determined by using 4,6-diamidino-2-phenylindole (DAPI) and methyl green, which are known to bind to DNA at minor groove and major groove, respectively [44,45]. Prior to the addition of the complex, no apparent inhibition of DNA damage is observed in presence of both DAPI and methyl green (Figs. 4c and 5c, lanes 5 and 6)

either in presence or absence of H_2O_2 suggesting that the titled cobalt(II) complexes do not interact with the CT DNA by groove binding mode.

3. Conclusions

We describe here six seven coordinated cobalt(II) complexes of two pentadentate ligands, 2,6-diacetylpyridine bis(acylhydrazone) bearing ester groups. The single crystal structure of the Co(II) complex **1** has revealed a distorted pentagonal-bipyramidal geometry. The equatorial plane of the bipyramid is occupied by the pentadentate N_3O_2 2,6-diacetylpyridine bis(ethyl 2-(4-hydrazinecarbonyl)phenoxy)acetate) ligand while two dimethylformamide molecules occupy the axial position of the complex. The binding behaviors of the complexes with CT DNA were investigated by using absorption spectroscopy. The results indicate that the complexes could bind to CT DNA via intercalation. Further, viscosity study offers further support for the intercalative mode of binding of these cobalt(II) complexes. The cobalt(II) complexes **1** and **2** exhibit efficient nuclease activity in the presence and absence of hydrogen peroxide which has strong dependence on the concentration of complex as well as the reaction time. The hydroxyl radical scavenger effectively inhibits DNA cleavage mediated by the Co(II) complexes **1** and **2** either in the presence absence of H_2O_2 . These observations seem to suggest that the cobalt(II) complexes promote cleavage activity of pBR 322 plasmid DNA by oxidative cleavage mechanism. However, further studies warrant elucidating the detailed mechanisms of the Co(II) complex-mediated DNA cleavage. Results obtained from this study would be useful in the design of more effective and useful seven-coordinated transition metal complexes for DNA interactions.

4. Experimental Section

4.1. Material and methods

All the reagents and solvents were of reagent grade quality and were purchased from commercial suppliers. 4-Hydroxybenzohydrazide was synthesized by refluxing ethyl 4-hydroxybenzoate with excess hydrazine hydrate. Calf thymus DNA (CT-DNA) was purchased from Sigma- Aldrich. pBR 322 DNA was purchased from Fermentas. ^1H and ^{13}C NMR spectra were recorded on a Bruker 400 MHz spectrometer in DMSO-d_6 with

TMS as the internal standard. IR spectra were recorded on pure solid samples with a Thermo-Scientific, Nicolet iS10-ATR. The electronic spectra of the compounds were recorded on a PG Instruments T80+ UV/Vis Spectrophotometer. Carbon, hydrogen and nitrogen analyses were carried out on a LECO 932 CHNS analyzer and cobalt content was determined by atomic absorption spectroscopy using the DV 2000 Perkin Elmer ICP-AES. Room temperature magnetic susceptibility measurements were carried out on powdered samples using a Sherwood Scientific MK1 Model Gouy Magnetic Susceptibility Balance. The preparation of 2,6-diacetylpyridine bis(4-hydroxybenzoylhydrazone) has been described previously [27].

4.2. Synthesis of 2,6-diacetylpyridine bis(4-ethoxyacetatebenzoylhydrazone) (H_2L^1)

Ethyl bromoacetate (2 mmol, 0.334 g) was added to a mixture of 2,6-diacetylpyridine bis(4-hydroxybenzoylhydrazone) (1 mmol, 0.431 g) and dry K_2CO_3 (2 mmol, 0.276 g) in 25 mL acetone with catalytic amount of KI. The reaction mixture was refluxed with stirring for 24 hours and poured to ice water. The white precipitate formed was filtered and washed with water and finally recrystallized from methanol. Yield 68 %; Mp 107 °C; UV (DMF, nm) 214, 312, IR (ATR, cm^{-1}) 3282 (NH), 2998-2911 (CH)_{aliphatic}, 1758 (C=O)_{ester}, 1651 (C=O)_{amide}, 1604 (C=N), 1385 (C-N), 1256 and 1176 (C-O-C); 1H NMR (DMSO- d_6 , ppm) δ 1.24 (t, 6H, CH_3), 2.55 (s, 3H, N=C- CH_3), 4.21 (q, 4H, OCH_2CH_3), 4.92 (s, 4H, Ar- OCH_2) and 4.87 (s, 2H, Ar- OCH_2), 7.08 (d, 4H, ArH), 7.91, (d, 4H, ArH), 8.10 (m, 3H, ArH), 10.80 (s, 2H, NH); ^{13}C NMR (DMSO- d_6 , ppm) 168.4 (C=O)_{ester}, 160.2 (C=O)_{amide}, 154.2 (C-O), 142.1 (C=N), 137.1, 130.7, 130.2, 129.9, 126.6, 120.4, 114.1 (Ar-C), 64.6 (COO $\underline{C}H_2$) and 60.7 (O $\underline{C}H_2$), 14.6 ($\underline{C}H_3$ -C=N), 12.3 ($\underline{C}H_3CH_2$). Analysis (%Calculated/found) for $C_{31}H_{33}N_5O_8$; C: 61.68/61.90, H: 5.51/5.40, N: 11.60/11.37.

4.3. Synthesis of 2,6-diacetylpyridine bis(4-ethoxybutyratebenzoylhydrazone) (H_2L^2)

Ethyl 4-bromobutyrate (2 mmol, 0.429 g) was added to a suspension of 2,6-diacetylpyridine bis(4-hydroxybenzoylhydrazone) (1 mmol, 0.431 g) and dry K_2CO_3 (2 mmol, 0.276 g) in DMF (10 mL) with catalytic amount of KI. The reaction mixture was refluxed with stirring for 4 hours and poured to 200 mL of ice water. The white precipitate formed was filtered and washed with water and finally recrystallized from

ethanol. Yield 70 %; Mp 165 °C; UV (MeOH, nm) 216, 295 sh, 316, IR (ATR, cm^{-1}) 3273 (NH), 2977-2922 (CH)_{aliphatic}, 1731 (C=O)_{ester}, 1654 (C=O)_{amide}, 1606 (C=N), 1372 (C-N), 1247 and 1172 (C-O-C); ^1H NMR (DMSO- d_6 , ppm) δ 1.20 (t, 6H, CH_3), 2.02 (qui, 4H, $\text{CH}_2\text{CH}_2\text{CH}_2$), 2.55 (s, 6H, N=C-CH_3), 2.49 (4H, COCH_2), 4.10 (m, 8H, OCH_2), 7.05 (d, 4H, ArH), 7.91, (d, 4H, ArH), 8.10 (m, 3H, ArH), 10.77 (s, 2H, NH); ^{13}C NMR (DMSO- d_6 , ppm) 170.4 (C=O)_{ester}, 161.7 (C=O)_{amide}, 152.6 (C-O), 142.6 (C=N), 137.7, 134.9, 130.7, 126.6, 129.9, 124.6, 123.6, 114.5 (Ar-C), 68.2, 61.4, 30.3, 24.1, 14.1, 12.6 ($\text{C}_{\text{Aliphatic}}$). Analysis (%Calculated/found) for $\text{C}_{31}\text{H}_{33}\text{N}_5\text{O}_8$: C: 63.72/63.89, H: 6.26/6.70, N: 10.62/10.78

4.4. Synthesis of Co(II) complexes

4.4.1. $[\text{Co}(\text{L}^n)\text{X}_2]$ ($n=1$, $\text{X}=\text{DMF}$ for **1**; $n=2$, $\text{X}=\text{H}_2\text{O}$ for **2**)

A solution of $(\text{CH}_3\text{COO})_2\text{Co}\cdot 4\text{H}_2\text{O}$ (0.249 g, 1 mmol) in MeOH (10 ml) was added by dropwise to suspension of the ligand (1 mmol) in 50 ml MeOH. The reaction mixture was refluxed for 3 h. The precipitated orange complex was filtered off, washed with water and methanol. In the case of the complex **1**, the crystals suitable for X-ray diffraction were obtained upon diffusion of the ethyl ether into the DMF solution.

For $[\text{Co}(\text{L}^1)(\text{DMF})_2]$ (**1**)

Yield: 81%; m.p.: 170 °C. $\mu_{\text{eff}} = 4.22$ B.M.; UV (DMF, nm) 268, 352, 411 (sh); FT-IR (ATR, cm^{-1}) 1763 s (C=O), 1603 m (C=N-N=C), 1262 s (C-O). Analysis (%Calculated/found) for $\text{C}_{37}\text{H}_{45}\text{CoN}_7\text{O}_{10}$: C: 55.09/55.20, H: 5.62/5.50, N: 12.15/11.95, Co: 7.31/7.25.

For $[\text{Co}(\text{L}^2)(\text{H}_2\text{O})_2]$ (**2**)

Yield: 81%; m.p.: 190 °C. $\mu_{\text{eff}} = 4.31$ B.M.; UV (DMF, nm) 270, 350, 400 (sh); FT-IR (ATR, cm^{-1}) 3383 b (O-H), 1728 s (C=O), 1603 (C=N-N=C), 1246 s (C-O). Analysis (%Calculated/found) for $\text{C}_{35}\text{H}_{43}\text{CoN}_5\text{O}_{10}$: C: 55.85/55.60, H: 5.76/5.44, N: 9.30/9.06, Co: 7.83/7.39.

4.4.2. $[\text{Co}(\text{H}_2\text{L}^n)\text{Y}_2]$ ($n=1$ or 2 ; $\text{Y}=\text{N}_3^-$ (**3** and **4**) or NCS^- (**5** and **6**))

A solution of $(\text{CH}_3\text{COO})_2\text{Co}\cdot 4\text{H}_2\text{O}$ (0.249 g, 1 mmol) in MeOH (10 ml) was added by dropwise to suspension of the ligand (1 mmol) in 50 ml MeOH. After the mixture was refluxed for 0.5 h, an aqueous solution of KSCN (0.194 g, 2 mmol in 5 ml) or NaN_3 (0.130 g, 2 mmol) was added, and the resulting mixture was refluxed for further 3 h. The precipitate was filtered off, washed with methanol and diethyl ether several times, and dried in vacuum.

For $[\text{Co}(\text{H}_2\text{L}^1)(\text{N}_3)_2]$ (3)

Red complex; yield: 74%; m.p.: 310 °C. $\mu_{\text{eff}} = 4.25$ B.M.; UV (DMF, nm) 272, 350, 422 (sh); FT-IR (ATR, cm^{-1}) 3421 w (N-H), 2046 s and 1297 w (N=N=N), 1751 s and 1638 m (C=O), 1601 m (C=N), 1265 s (C-O). Analysis (%Calculated/found) for $\text{C}_{31}\text{H}_{33}\text{CoN}_{11}\text{O}_8$; C: 49.87/50.05, H: 4.46/4.68, N: 20.64/20.21, Co: 7.89/7.66.

For $[\text{Co}(\text{H}_2\text{L}^2)(\text{N}_3)_2]$ (4)

Brown complex; yield: 77%; m.p.: <350 °C. $\mu_{\text{eff}} = 4.20$ B.M.; UV (DMF, nm) 270, 352, 402 (sh); FT-IR (ATR, cm^{-1}), 3383 w (N-H), 2034 s and 1273 s (N=N=N), 1724 and 1627 s (C=O), 1604 m (C=N), 1244 s (C-O). Analysis (%Calculated/found) for $\text{C}_{35}\text{H}_{41}\text{CoN}_{11}\text{O}_8$; C: 52.37/52.54, H: 5.15/5.23, N: 19.19/19.36, Co: 7.34/7.49.

For $[\text{Co}(\text{H}_2\text{L}^1)(\text{NCS})_2]$ (5)

Red complex; yield: 79%; m.p.: 230 °C. $\mu_{\text{eff}} = 4.25$ B.M.; UV (DMF, nm) 270, 348, 416 (sh); FT-IR (ATR, cm^{-1}) 3383 w (N-H), 2050 m and 902 w (S=C=N), 1751 s and 1640 m (C=O), 1603 (C=N), 1242 s C-O). Analysis (%Calculated/found) for $\text{C}_{33}\text{H}_{33}\text{CoN}_7\text{O}_8\text{S}_2$; C: 50.90/50.37, H: 4.27/4.31, N: 12.59/12.40, S: 8.23/8.62, Co: 7.57/7.49.

For $[\text{Co}(\text{H}_2\text{L}^2)(\text{NCS})_2]$ (6)

Red complex; yield: 75%; m.p.: 315 °C. $\mu_{\text{eff}} = 4.21$ B.M.; UV (DMF, nm) 268, 350, 406 (sh); FT-IR (ATR, cm^{-1}) 3440 w (N-H), 2078 s and 940 w (S=C=N), 1721 s and 1645 m (C=O), 1602 (C=N), 1252 s C-O). Analysis (%Calculated/found) for $\text{C}_{37}\text{H}_{41}\text{CoN}_7\text{O}_8\text{S}_2$; C: 53.23/53.41, H: 4.95/4.76, N: 11.74/11.38, S: 7.68/7.77, Co: 7.06/7.21.

4.5. X-ray Diffraction Study

Crystallographic data were recorded on a Bruker Smart Breeze CCD area-detector diffractometer using MoK α radiation ($\lambda=0.71073$ Å) at T=296 (2) K [46]. Absorption corrections by multi-scan were applied [47] Cell refinement was carried out using Bruker SAINT and data was reduced by using Bruker SAINT [48]. The structure was solved using SHELXS97 [47] and refined using SHELXL2013 [48] by full-matrix least-squares on F² against ALL reflections. The weighted R-factor wR and goodness of fit S are based on F². The threshold expression of F² > 2sigma(F²) is used only for calculating R-factors. All estimated standard deviations (e.s.d.'s) are calculated using the full covariance matrix. The cell e.s.d.'s are taken into account individually in the estimation of e.s.d.'s in distances, angles, and torsion angles; correlations between e.s.d.'s in cell parameters are only used when they are defined by crystal symmetry. Molecular graphics were drawn ORTEP-3 [49], PLATON [50] and the material for publication prepared using WinGX [51]. All non-hydrogen atoms were refined anisotropically and hydrogen atoms were added according to the theoretical model. The fractional atomic coordinates are given in Table S1, supporting information.

4.6. DNA Binding

4.6.1. Electronic absorption titrations

All the experiments involving the interaction of the complexes with CT-DNA were carried out in water buffer containing 5 mM tris [tris(hydroxymethyl)aminomethane] and 50 mM NaCl, and adjusted to pH 7.3 with HCl. The solution of CT-DNA in the buffer gave a ratio of UV absorbance of 1.8 –1.9:1 at 260 and 280 nm, indicating that the CT-DNA was sufficiently free of protein [52]. The CT-DNA concentration per nucleotide was determined spectrophotometrically by employing an extinction coefficient of 6600 M⁻¹ cm⁻¹ at 260 nm [53]. An appropriate amount of the cobalt complex was dissolved in a solvent mixture of 1% DMF and 99% tris–HCl buffer. Absorption titration experiments were performed by maintaining the metal complex concentration as constant while gradually increasing the concentration of the CT-DNA within 0-80 μM.

4.6.2. Viscosity measurements

Viscosity experiments were carried out using an Ubbelodhe viscometer at room temperature. The viscosity of CT-DNA solution (25 μM) was measured in the absence and presence of increasing amounts of the complex (6,25-50 μM) in tris-HCl buffer (10 mM tris-HCl-NaCl; pH=7.6) containing %5 DMF solution. Flow time was measured three times with a digital stopwatch. Viscosity values were presented as $(\eta/\eta_0)^{1/3}$ versus concentrations of [complex]/[DNA] [28,38] where η was the viscosity value for DNA in presence of the cobalt(II) complex and η_0 was the viscosity value of CT-DNA alone.

4.7. Chemical nuclease activity

pBR 322 plasmid DNA was used for all cleavage activities [28,38,39,43]. In a typical experiment, 2 μL plasmid DNA (0.50 $\mu\text{g}/\mu\text{L}$) was mixed with different concentration of the cobalt(II) complex (25, 50, 75, 100 and 200 μM) dissolved in DMF to determine optimum activation concentration. In the case of oxidative cleavage, 5 μL H_2O_2 (5 mM) was added to mixture to oxidize the reactant. Finally the reaction mixture was diluted with the Tris buffer (100 mM Tris, pH: 8) to a total volume of 30 μL . After that reaction mixtures were incubated at 37 $^\circ\text{C}$ for two hours. Samples (20 μL) were then loaded with 4 μL loading dye (0.25% bromophenol blue, 0.25% xylene cyanol, 30% glycerol, 10 mmol EDTA) on a %1 agarose gel containing 1 $\mu\text{g}/\text{mL}$ of EtBr. The gel was run at 100 V for 3 h in TBE buffer and photographed under UV light. To test for the presence of reactive oxygen species generated during strand scission, reactive oxygen intermediate scavengers, that is, SOD, DMSO and NaN_3 were added alternately to the reaction mixture and the samples were treated as described above.

Acknowledgements

This work was funded by the Scientific and Technological Research Council of Turkey (TÜBİTAK, TBAG-112T315).

Appendix A. Supplementary data

X-ray crystallographic files of the cobalt(II) complex (**1**) are available. These data can be obtained free of charge via www.ccdc.cam.ac.uk/conts/retrieving.html (or from the CCDC, 12 Union Road, Cambridge CB2 1EZ, UK; fax: +44 1223 336033; email:

deposit@ccdc.cam.ac.uk). Supplementary data associated with this article can be found, in the online version.

References

- [1] K. E. Erkkila, D. T. Odom, J. K. Barton, *Chem. Rev.* 99 (1999) 2777.
- [2] J. K. Barton, A. L. Raphael, *J. Am. Chem. Soc.* 106 (1984) 2466.
- [3] P. Melnyk, V. Leroux, C. Sergheraert, P. Grellier, C. Sergheraert, *Bioorg. Med. Chem. Lett.* 16 (2006) 31.
- [4] C. Cunha, J.M. Figueiredo, J. L. M. Tributino, A. L. P. Miranda, H. C. Castro, R. B. Zingali, C. A. M. Fraga, M. C. B. de Souza, V. F. Ferreira, E. Barreiro, *J. Bioorg. Med. Chem.* 11 (2003) 2051.
- [5] L. Savanini, L. Chiasserini, A. Gaeta, C. Pellerano, *Bioorg. Med. Chem.* 10 (2002) 2193.
- [6] S. Thyagarajan, N. N. Murthy, A. A. N. Sarjeant, K. D. Karlin, S. E. Rokita, *J. Am. Chem. Soc.* 128 (2006) 7003.
- [7] G. Barone, A. Terenzi, A. Lauria, A. M. Almerico, J. M. Leal, N. Busto, B. Garcia, *Coord. Chem. Rev.* 257 (2013) 2848.
- [8] R. Indumathy, M. Kanthimathi, T. Weyhermuller, B. U. Nair, *Polyhedron*, 27 (2008) 3443.
- [9] K. Jiao, Q. W. Wang, W. Sun, F. F. Jian, *J. Inorg. Biochem.* 99 (2005) 1369.
- [10] R. Eshkourfu, B. Cobeljic, M. Vujcic, I. Turel, A. Pevec, K. Sepcic, M. Zec, S. Radulovic, T. Srdic-Radic, D. Mitic, K. Andjelkovic, D. Sladic. *J Inorg Biochem.* 105 (2011) 1196.
- [11] C. Gokce, R. Gup, *J. Photochem. Photobiol. B Biol.* 122 (2013) 15.
- [12] M. Ahmad, M. Afzal, S. Tabassum, B. Kalinska, J. Mrozinski, P.K. Bharadwaj, *Eur. J. Med. Chem.* 74 (2014) 683.
- [13] H. Lopez-Sandoval, M. E. Londono-lemos, R. Garza-Velasco, I. Poblano-Melendez, P. Granada- Macias, I. Gracia-Mora, N. Barba-Behrens *J. Inorg. Biochem.* 102 (2008) 1267.
- [14] N. Shahabadi, S. Kashanian, F. Darabi, *Eur. J. Med. Chem.* 45 (2010) 4239.
- [15] S. Sathiyaraj, K. Sampath, G. Raja, R.J. Butcher, S.K. Gupta, C. Jayabalakrishnan, *Inorg. Chim. Acta.* 406 (2013) 44.

- [16] R. Indumathy, S. Radhika, M. Kanthimathi, T. Weyhermuller, B. U. Nair, J. Inorg. Biochem. 101 (2007) 434.
- [17] A. Panja, Polyhedron 43 (2012) 22.
- [18] H. Gopinathan, N. Komathi, M. N. Arumugan, Inorg. Chim. Acta. 416 (2014) 93.
- [19] T. J. Giordano, G. J. Palenik, R. C. Palenik, D. A. Sullivan, Inorg. Chem. 18 (1979) 2445.
- [20] R. Ruamps, L. J. Batchelor, R. Maurice, N. Gogoi, P. Jiménez-Lozano, N. Guihéry, C. de Graaf, A. L. Barra, J.P. Sutter, T. Mallah, Chem.-Eur. J. 19 (2013) 950.
- [21] M. Carcelli, P. Mazza, G. Pellizzi, F. Zani, J. Inorg. Biochem. 57 (1995) 43.
- [22] A. I. Matesanz, I. Leitao, P. Souza, J. Inorg. Biochem. 125 (2013) 26.
- [23] M. Kozłowski, R. Kierzek, M. Kubicki, W. Radecka-Paryzek, J. Inorg. Biochem. 126 (2013) 38.
- [24] B. Bottari, R. Maccari, F. Monforte, R. Ottana, M. G. Vigorita, G. Bruno, F. Nicola, A. Rotondo, E. Rotondo, Bioorg. Med. Chem. 9 (2001) 2203-2211.
- [25] I. Ivanovic-Burmazovic, A. Bacchi, G. Pelizzi, V. M. Leovac, K. Andjelkovic, Polyhedron. 18 (1999) 119.
- [26] K. S. O. Ferraz, N. F. Silva, J.G. da Silva, L. F. de Miranda, C. F. D. Romeiro, E. M. Souza-Fagundes, I. C. Mendes, H. Beraldo, Eur. Med. Chem. 53 (2012) 98.
- [27] N. Dilek, B. Güneş, O. Büyükgüngör, R. Gup, Crystallogr. Rep+. 58 (2013) 98.
- [28] R. Gup, C. Gokce, S. Akturk, Spectrochim. Acta A. 134 (2015) 484.
- [29] C. Gökce, R. Gup, Appl. Organometall. Chem. 27 (2013) 263.
- [30] M. J. Li, T.Y. Lan, Z.S. Lin, C. Yi, G. N. Chen, J. Biol. Inorg. Chem. 18 (2013) 993.
- [31] A. A. R. Despaigne, J. G. da Silva, A. C. M. do Carmo, F. Sives, O. E. Piro, E. E. Castellano, H. Beraldo, Polyhedron 28 (2009) 3797.
- [32] J. K. Barton, A. T. Danishhefsky, J. M. Goldberg, J. Am. Chem. Soc. 106 (1984) 2172.
- [33] T. Hirohama, Y. Kuranuki, E. Ebina, T. Sugizaki, H. Arii, M. Chikira, P. T. Selvi, M. J. Palaniandavar, Inorg. Biochem. 99 (2005) 1205.

- [34] J. K. Barton, J. J. Dannenberg, A. L. Raphael, *J. Am. Chem. Soc.* 104 (1982) 4967.
- [35] S. Ramakrishnan, E. Suresh, A. Riyasdeen, M. A. Akbarsha, M. Palaniandavar, *Dalton Trans.* 40 (2011) 3245.
- [36] D. Lahiri, S. Roy, S. Saha, R. Majumdar, R. R. Dighe, A. R. Chakravarty, *Dalton Trans.* 39 (2010) 1807.
- [37] S. Satyanarayana, J. C. Dabrowiak, J. B. Chaires, *Biochem.* 31 (1992) 9319.
- [38] G. Cohen, H. Einsenberg, *Biopolymers* 8 (1969) 45.
- [39] S. S. Massoud, R. S. Perkins, F. R. Louka, W. Xu, A. L. Roux, Q. Dutercq, R. C. Fischer, F. A. Mautner, M. Handa, Y. Hiraoka, G. L. Kreft, T. Bortolotto, H. Terenzi, *Dalton Trans.* 43 (2014) 10086.
- [40] W. Xu, J. A. Craft, P. R. Fontenot, M. Barends, K. D. Knierim, J. H. Albering, F. A. Mautner, S. S. Massoud, *Inorg. Chim. Acta* 373 (2011) 159.
- [41] J. Qian, X.F. Ma, J.L. Tian, W. Gu, J. Shang, X. Liu, SP. Yan, *J. Inorg. Biochem.* 104 (2010) 993.
- [42] N. J. Garrido, L. Perello, R. Ortiz, *J. Inorg. Biochem.* 99 (2005) 677.
- [43] S. S. Massoud, K. T. Broussard, F. A. Mautner, R. Vicente, M. K. Saha, I. Bernal, *Inorg. Chim Acta* 361 (2008) 123.
- [44] E. Trotta, N. D. Grosso, M. Erba, M. Paci, *Biochem.* 39 (2000) 6799.
- [45] X. Dong, X. Wang, M. Lin, H. Sun, X. Yang, Z. Guo, *Inorg. Chem.* 49 (2010) 2541.
- [46] Bruker, APEX2, SAINT and SADABS, Bruker AXS Inc., 2005, Madison, Wisconsin, USA.
- [47] R. H. Blessing, *Acta Cryst.* A51 (1995) 33.
- [48] G. M. Sheldrick, *Acta Cryst.* A64 (2008) 112.
- [49] L. J. Farrugia, *Appl. Cryst.* 30 (1997) 565.
- [50] A. L. Spek, PLATON. Multipurpose Crystallographic Tool, 1998, Utrecht University.
- [51] L. J. Farrugia, *Appl. Cryst.* 32 (1999) 837.
- [52] J. Marmur, *J. Mol. Biol.* 3 (1961) 208.
- [53] A. M. Pyle, J. P. Rehmman, J. P. Meshoyrer, C. V. Kumar, N. J. Turro, J.K. Barton, *J. Am. Chem. Soc.* 111 (1989) 3053.

Figure Captions

Fig. 1. An ORTEP drawing of molecular structure with the crystallographic numbering scheme. Thermal ellipsoids are drawn at % 30 probability levels.

Fig. 2. Absorption spectra of the complex (1) with increasing concentration of CT-DNA. [Complex] = 25 μ M, [DNA] = 0–80 μ M.

Fig. 3. Effect of increasing amounts of the cobalt(II) complex (1), DAPI and EB on the relative viscosity of calf thymus DNA at room temperature.

Fig. 4. (a) Agarose gel electrophoresis patterns of plasmid pBR 322 DNA after 2 h incubation with various concentrations of complex (1) in the presence of H₂O₂. Lane 1, 1 (200 μ M) + DNA + H₂O₂; Lane 2, 1 (100 μ M) + DNA + H₂O₂; Lane 3, 1 (75 μ M) + DNA + H₂O₂; Lane 4, 1 (50 μ M) + DNA + H₂O₂; Lane 5, 1 (25 μ M) + DNA + H₂O₂; Lane 6, DNA control. **(b)** Reaction time dependence of the oxidative DNA cleavage of complexes (1), 1 (100 μ M). Lane 7, DNA control; the reaction time for lanes 1-6 is 1, 2, 3, 4, 5, 6h, respectively. **(c)** Oxidative plasmid pBR 322 DNA cleavage in the presence of different scavengers and presence of different groove binding after 2 h incubation with of complex (1). Lane 1, 1 (100 μ M) + DNA + H₂O₂; Lane 2, 1 (100 μ M) + DNA + H₂O₂ + DMSO; Lane 3, 1 (100 μ M) + DNA + H₂O₂ + SOD; Lane 4, 1 (100 μ M) + DNA + H₂O₂ + NaN₃; Lane 5, 1 (100 μ M) + DNA + H₂O₂ + DAPI; Lane 6, 1 (100 μ M) + DNA + H₂O₂ + methyl green; Lane 7, DNA control.

Fig. 5. (a) Agarose gel electrophoresis patterns of plasmid pBR 322 DNA after 3 h incubation with various concentrations of complexes (1) in the absence of H₂O₂. Lane 1, 1 (200 μ M) + DNA; Lane 2, 1 (100 μ M) + DNA; Lane 3, 1 (75 μ M) + DNA; Lane 4, 1 (50 μ M) + DNA; Lane 5, 1 (25 μ M) + DNA; Lane 6, DNA control. **(b)** Reaction time dependence of the hydrolytic DNA cleavage by the complexes (1), 1 (100 μ M). Lane 7, DNA control; the reaction time for lanes 1-6 is 1, 2, 3, 4, 5, 6h, respectively; **(c)** Hydrolytic plasmid pBR 322 DNA cleavage in the presence of different scavengers and presence of different groove binding after 3 h incubation with of complexes (1). Lane 1, 1 (75 μ M) + DNA; Lane 2, 1 (75 μ M) + DNA + DMSO; Lane 3, 1 (75 μ M) + DNA + SOD; Lane 4, 1 (75 μ M) + DNA + NaN₃; Lane 5, 1 (75 μ M) + DNA + DAPI; Lane 6, 1 (75 μ M) + DNA + methyl green; Lane 7, DNA control.

Fig. S1. A packing diagram for molecule, projected along *a* direction. Hydrogen bonds are indicated by dashed lines.

Fig. S2. Absorption spectra of the complex (2) with increasing concentration of CT-DNA. [Complex] = 25 μ M, [DNA] = 0–80 μ M.

Fig. S3. Absorption spectra of the complex (3) with increasing concentration of CT-DNA. [Complex] = 25 μ M, [DNA] = 0–80 μ M.

Fig. S4. Absorption spectra of the complex (4) with increasing concentration of CT-DNA. [Complex] = 25 μ M, [DNA] = 0–80 μ M.

Fig. S5. Absorption spectra of the complex (5) with increasing concentration of CT-DNA. [Complex] = 25 μ M, [DNA] = 0–80 μ M.

Fig. S6. Absorption spectra of the complex (6) with increasing concentration of CT-DNA. [Complex] = 25 μ M, [DNA] = 0–80 μ M.

Fig. S7. Effect of increasing amounts of the cobalt(II) complex (2), DAPI and EB on the relative viscosity of calf thymus DNA at room temperature.

Fig. S8. Effect of increasing amounts of the cobalt(II) complex (3), DAPI and EB on the relative viscosity of calf thymus DNA at room temperature.

Fig. S9. Effect of increasing amounts of the cobalt(II) complex (4), DAPI and EB on the relative viscosity of calf thymus DNA at room temperature.

Fig. S10. Effect of increasing amounts of the cobalt(II) complex (5), DAPI and EB on the relative viscosity of calf thymus DNA at room temperature.

Fig. S11. Effect of increasing amounts of the cobalt(II) complex (6), DAPI and EB on the relative viscosity of calf thymus DNA at room temperature.

Fig. S12. (a) Agarose gel electrophoresis patterns of plasmid pBR 322 DNA after 2 h incubation with various concentrations of complex (2) in the presence of H₂O₂. Lane 1, 2 (200 μ M) + DNA + H₂O₂; Lane 2, 2 (100 μ M) + DNA + H₂O₂; Lane 3, 2 (75 μ M) + DNA + H₂O₂; Lane 4, 2 (50 μ M) + DNA + H₂O₂; Lane 5, 2 (25 μ M) + DNA + H₂O₂; Lane 6, DNA control. (b) Reaction time dependence of the oxidative DNA cleavage of complexes (2), 2 (100 μ M). Lane 7, DNA control; the reaction time for lanes 1-6 is 1, 2, 3, 4, 5, 6h, respectively. (c) Oxidative plasmid pBR 322 DNA cleavage in the presence of different scavengers and presence of different groove binding after 2 h incubation with of complex (2). Lane 1, 2 (100 μ M) + DNA + H₂O₂; Lane 2, 2 (100 μ M) + DNA + H₂O₂ + DMSO; Lane 3, 2 (100 μ M) + DNA + H₂O₂ + SOD; Lane 4, 2 (100 μ M) + DNA + H₂O₂ + NaN₃; Lane 5, 2 (100 μ M) + DNA + H₂O₂ + DAPI; Lane 6, 2 (100 μ M) + DNA + H₂O₂ + methyl green; Lane 7, DNA control.

Fig. S13. (a) Agarose gel electrophoresis patterns of plasmid pBR 322 DNA after 3 h incubation with various concentrations of complexes (**2**) in the absence of H₂O₂. Lane 1, **2** (200 μM) + DNA; Lane 2, **2** (100 μM) + DNA; Lane 3, **2** (75 μM) + DNA; Lane 4, **2** (50 μM) + DNA; Lane 5, **2** (25 μM) + DNA; Lane 6, DNA control. **(b)** Reaction time dependence of the hydrolytic DNA cleavage by the complexes (**2**), **2** (100 μM). Lane 7, DNA control; the reaction time for lanes 1-6 is 1, 2, 3, 4, 5, 6h, respectively; **(c)** Hydrolytic plasmid pBR 322 DNA cleavage in the presence of different scavengers and presence of different groove binding after 3 h incubation with of complexes (**2**). Lane 1, **2** (50 μM) + DNA; Lane 2, **2** (50 μM) + DNA + DMSO; Lane 3, **2** (50 μM) + DNA + SOD; Lane 4, **2** (50 μM) + DNA + NaN₃; Lane 5, **2** (50 μM) + DNA + DAPI; Lane 6, **2** (50 μM) + DNA + methyl green; Lane 7, DNA control.

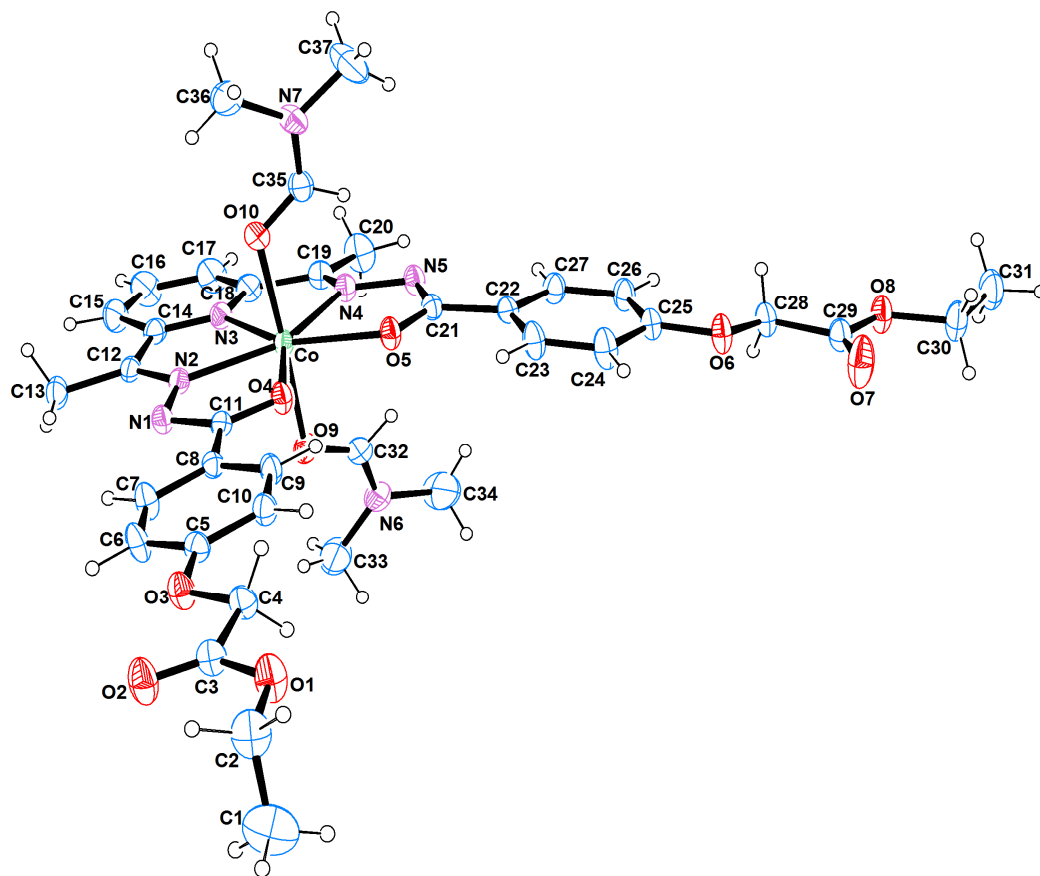


Fig. 1.

ACCEPTED

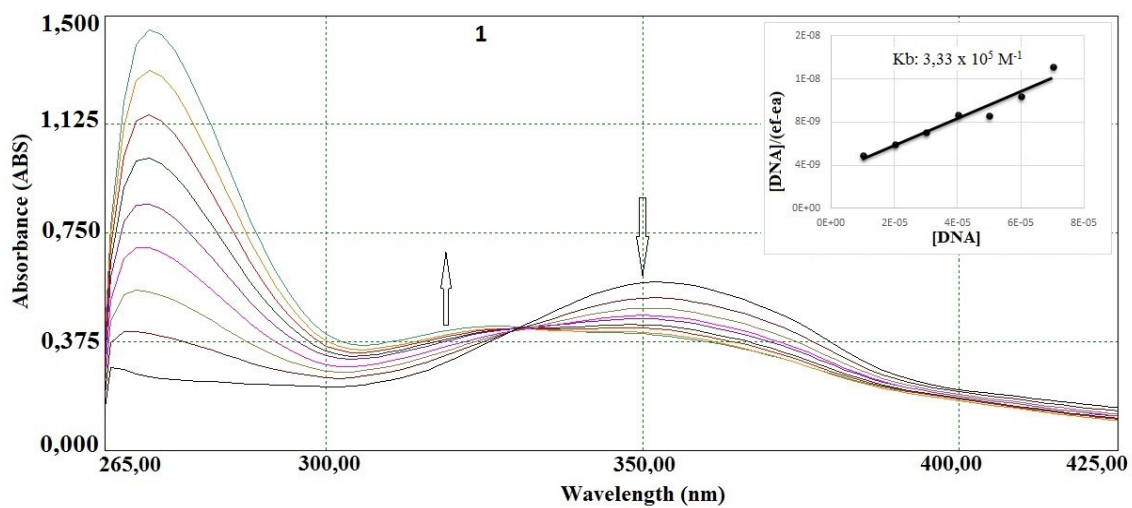


Fig. 2.

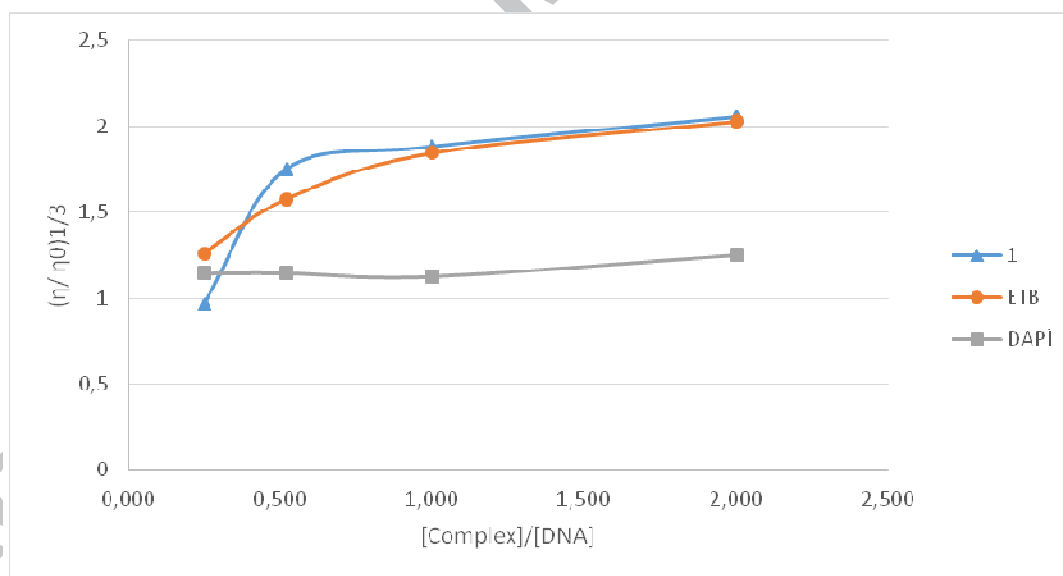


Fig. 3.

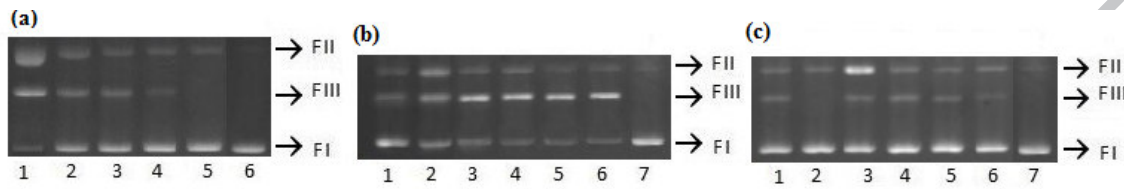


Fig. 4.

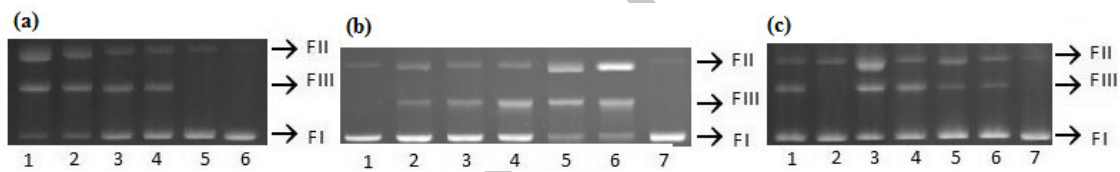


Fig. 5.

Table 1

Crystallographic data and structural refinement for the cobalt(II) complex

Chemical Formula	Co[C ₃₁ H ₃₁ N ₅ O ₈].2(C ₃ H ₇ NO)
Formula weight (amu)	806.73
Crystal form, color	prism, orange
Crystal size (mm)	0.590 x 0.240 x 0.140
Crystal system	Triclinic
Space group	<i>P</i> -1
<i>a</i> (Å)	8.9694 (7)
<i>b</i> (Å)	14.6496 (11)
<i>c</i> (Å)	15.0420 (11)
α (°)	90.208 (4)
β (°)	92.544 (4)
γ (°)	92.799 (4)
<i>V</i> (Å ³)	1956.2 (3)
<i>Z</i>	2
<i>D</i> _x (g/cm ³)	1.370
λ (MoK α) Å	0.71073
μ (MoK α) mm ⁻¹	0.590
<i>T</i> (K)	296(2)
θ _{max}	26.372
θ _{min}	1.36
H	-11---11
K	-18----18
L	-18----18
Number of reflections measured	45920
Number of independent reflections	7978
Number of reflections [<i>I</i> > 2 σ (<i>I</i>)]	6041
Number of parameters	505
<i>R</i>	0.0427
<i>R</i> _w	0.0978
<i>S</i>	1.037
Weighting scheme,	1/[$\sigma^2(F_o^2) + (0.1040P)^2$ P = (F _o ² + 2F _c ²)/3
(Δ/σ) _{max}	0.050
($\Delta\rho$) _{max} , ($\Delta\rho$) _{min} (eÅ ⁻³)	0.299, -0.231
Measurements	Bruker APEXII
Structure determination	direct method (SHELXS-97)
Refinement	full matrix l.s. (SHELXL-2013)
Treatment of hydrogen atoms	geometric calculation

Table 2

Selected bond lengths (Å), bond angles (°) and torsion angles (°) of the cobalt(II) complex.

<i>Bond lengths</i>		<i>Bond angles</i>		<i>Torsion angles</i>			
Co–O4	2.129(2)	O4–Co–O5	77.44(5)	C35–O10–Co	120.1(2)	Co–O5–C21–N5	5.9(3)
Co–O5	2.154(1)	O4–Co–N2	71.98(6)	C12–N2–N1	118.4(2)	Co–O5–C21–C22	-170.7(1)
Co–O9	2.272(2)	O5–Co–N2	149.42(6)	C12–N2–Co	122.7(2)	O4–C11–C8–C9	4.9(3)
Co–O10	2.209(2)	O4–Co–N3	142.95(6)	N1–N2–Co	118.9(1)	N1–C11–C8–C7	4.4(3)
Co–N2	2.157(2)	O5–Co–N3	139.57(6)	C25–O6–C28	116.8(2)	Co–N2–C12–C14	2.8(2)
Co–N3	2.203(2)	N2–Co–N3	70.99(7)	C32–O9–Co	116.3(2)	C4–O3–C5–C10	-3.6(3)
Co–N4	2.230(2)	O4–Co–O10	88.51(6)	C11–N1–N2	108.4(2)	C28–O6–C25–C26	-7.5(3)
N2–N1	1.374(2)	O5–Co–O10	90.56(6)	C29–O8–C30	116.4(2)	C28–O6–C25–C24	171.4(2)
N4–N5	1.383(2)	N2–Co–O10	88.89(6)	C3–O1–C2	117.8(2)	O2–C3–C4–O3	-5.2(3)
		N3–Co–O10	91.92(6)	C19–N4–N5	118.1(2)	C18–N3–C14–C15	-2.6(3)
		O4–Co–N4	147.41(6)	C19–N4–Co	121.8(2)	Co–N4–C19–C18	9.1(3)
		O5–Co–N4	69.99(6)	N5–N4–Co	119.0(1)	Co–N4–C19–C20	-167.7(2)
		N2–Co–N4	140.57(7)	C21–N5–N4	107.9(2)	N4–C19–C18–N3	-4.2(3)
		N3–Co–N4	69.59(6)	C14–N3–C18	120.5(2)	C20–C19–C18–N3	172.7(2)
		O10–Co–N4	92.92(6)	C14–N3–Co	118.7(2)	C20–C19–C18–C17	-5.9(4)
		O4–Co–O9	93.19(6)	C18–N3–Co	120.7(1)	C30–O8–C29–O7	-2.9(4)
		O5–Co–O9	92.17(6)	O5–C21–N5	125.6(2)	O6–C28–C29–O7	6.3(4)
		N2–Co–O9	89.34(6)	O2–C3–O1	124.7(2)	O6–C28–C29–O8	-173.0(2)
		N3–Co–O9	85.27(6)	O10–C35–N7	125.8(2)	N3–C14–C15–C16	3.8(4)
		O10–Co–O9	177.04(6)	O7–C29–O8	124.0(2)	C12–C14–C15–C16	-173.6(2)
		N4–Co–O9	86.96(6)	O7–C29–C28	126.8(2)	Co–O9–C32–N6	-167.1(2)
		C11–O4–Co	115.4(1)	O8–C29–C28	109.2(2)	C33–N6–C32–O9	-3.5(5)
		C21–O5–Co	117.2(1)	O9–C32–N6	128.0(2)	N3–C18–C17–C16	2.8(4)
		C5–O3–C4	118.2(2)			C3–O1–C2–C1	97.5(3)

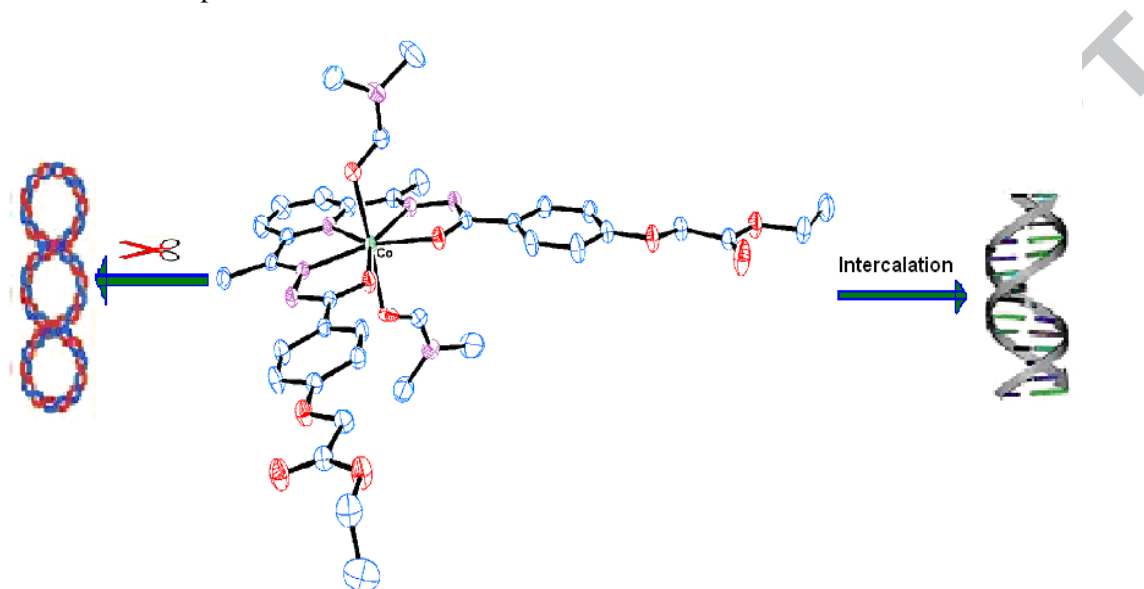
Note: Symmetry transformations: [#]-x, y, -z+1/2

Table 3

Effect of CT-DNA on the absorbance bands and binding constant of the complexes and adducts

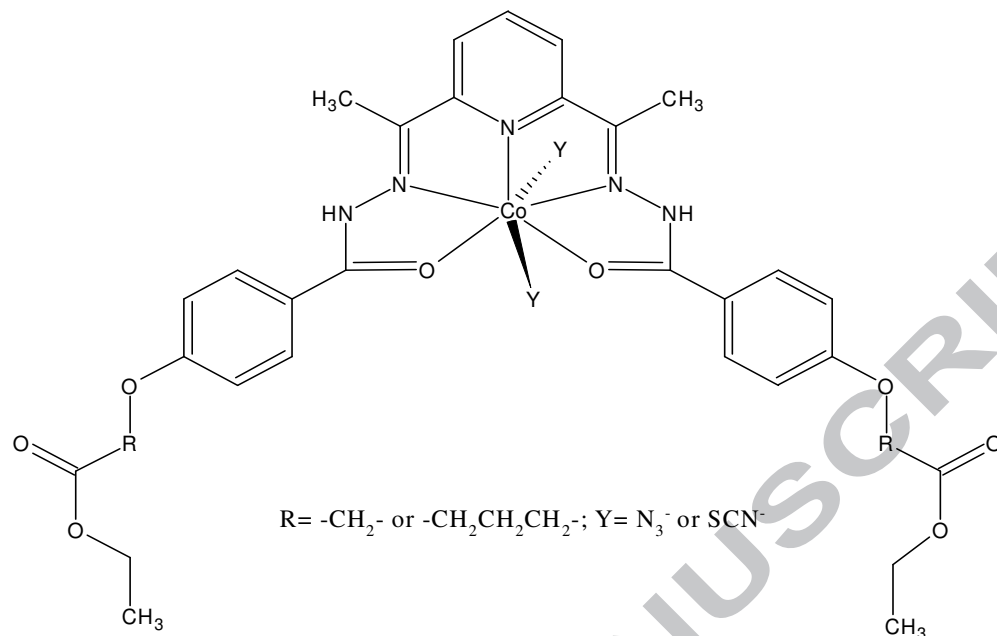
Complex	λ_{\max} (nm)		$\Delta\lambda$ (nm)	H (%)	$K_b(M^{-1})$
	Free	Bound			
1	352.0	348.0	4.0	26,29	3.33×10^5
2	350.0	346.0	4.0	8,99	2.33×10^5
3	350.0	348.0	2.0	13,89	2.50×10^5
4	352.0	350.0	2.0	10,13	1.67×10^5
5	348.0	346.0	2.0	11,11	1.00×10^5
6	350.0	348.0	2.0	11,79	2.00×10^5

The synthesis of a new series of seven-coordinated cobalt(II) complexes and their DNA interaction are reported.



Seven coordinated cobalt(II) complexes with 2,6-diacetylpyridine bis(4-acylhydrazone) ligands: Synthesis, characterization, DNA-binding and nuclease activity

Cansu Gökçe, Nefise Dilek and Ramazan Gup



A new series of pentadentate bis(4-acylhydrazones) based seven-coordinated cobalt(II) complexes, [Co(L)X₂] (X = DMF, H₂O) and [Co(H₂L)Y₂] (Y = N₃⁻ or NCS⁻), has been synthesized and characterized. Single crystal X-ray study of [Co(L¹)(DMF)₂] reveals that Co(II) complex has a pentagonal-bipyramidal coordination geometry. The cobalt(II) complexes bind to DNA through intercalation, and they are able to cleavage DNA both in the presence and absence of oxidant agent.

Highlights

- Six new seven-coordinated Co(II) complexes of pentadentate ligands have synthesized.
- $[\text{Co}(\text{L}^1)(\text{DMF})_2]$ has been structurally characterized.
- The cobalt(II) complexes bind with CT DNA through intercalation.
- The Co(II) complexes cleavage the pBR322 plasmid DNA *via* oxidative pathway.

ACCEPTED MANUSCRIPT